



1
2
3
4
5
6
7
8
9
10
11
12
13
14
15
16
17
18
19
20
21
22
23
24
25
26
27
28
29
30
31
32
33
34
35
36
37
38
39
40
41

Mg/Ca, Sr/Ca AND STABLE ISOTOPE FROM PLANKTONIC FORAMINIFERA
T. SACCULIFER: TESTING A MULTI-PROXY APPROACH FOR INFERRING
PALEO-TEMPERATURE AND PALEO-SALINITY

Delphine Dissard (1, 2), Gert Jan Reichart (3, 4), Christophe Menkes (5), Morgan Mangeas (5), Stephan Frickenhaus (2) and Jelle Bijma (2)

- (1) IRD/UMR LOCEAN (IRD-CNRS-MNHN-Sorbonne Université), Centre IRD de Nouméa 101 Promenade Roger Laroque, Nouméa 98848, New Caledonia.
- (2) Alfred-Wegener-Institute, Helmholtz-Zentrum für Polar- und Meeres Forschung, Am Handelshafen 12, 27570 Bremerhaven, Germany
- (3) NIOZ Royal Netherlands Inst. Sea Res, Den Burg, Texel, Netherlands.
- (4) Univ. Utrecht, Fac Geosci. Dept Earth Sci. Utrecht, Netherlands
- (5) IRD/UMR ENTROPIE (IRD, Univ. de la Réunion, CNRS, IFREMER, UNC), Centre IRD de Nouméa 101 Promenade Roger Laroque, Nouméa 98848, New Caledonia.

ABSTRACT

Over the last decades, sea surface temperature (SST) reconstructions based on the Mg/Ca of foraminiferal calcite have frequently been used in combination with the $\delta_{18}\text{O}$ signal from the same material, to provide estimates of $\delta_{18}\text{O}$ of the water ($\delta_{18}\text{O}_w$), a proxy for global ice volume and sea surface salinity (SSS). However, because of error propagation from one step to the next, better calibrations are required to increase accuracy and robustness of existing isotope and element to temperature proxy-relationships. Towards that goal, we determined Mg/Ca, Sr/Ca and the oxygen isotopic composition of *Trilobatus sacculifer* (previously referenced as *Globigerinoides sacculifer*), collected from surface waters (0-10m), along a North-South transect in the eastern basin of the tropical/subtropical Atlantic Ocean. We established a new paleo-temperature calibration based on Mg/Ca, and on the combination of Mg/Ca and Sr/Ca. Subsequently, a sensitivity analysis was performed in which, one, two, or three different equations were considered. Results indicate that foraminiferal Mg/Ca allow for an accurate reconstruction of surface water temperature. Combining equations, $\delta_{18}\text{O}_w$ can be reconstructed with a precision of about $\pm 0.5\%$. However, the best possible salinity reconstruction based on locally calibrated equations, only allowed reconstruction with an uncertainty of ± 2.49 . This was confirmed by a Monte Carlo simulation, applied to test successive reconstructions in an ‘ideal case’, where explanatory variables are known. This simulation shows that from a pure statistical point of view, successive reconstructions involving Mg/Ca and $\delta_{18}\text{O}_c$ preclude salinity



42 reconstruction with a precision better than ± 1.69 and hardly better than ± 2.65 , due to error
43 propagation. Nevertheless, a direct linear fit to reconstruct salinity based on the same measured
44 variables (Mg/Ca and $\delta^{18}O_c$) was established. This direct reconstruction of salinity lead to a
45 much better estimation of salinity (± 0.26) than the successive reconstructions.

46

47

48

I. INTRODUCTION

49

50 Since Emiliani's pioneering work (1954), oxygen isotope compositions recorded in fossil
51 foraminiferal shells became a major tool to reconstruct past sea surface temperature. After
52 Shackleton's seminal studies (1967, 1968 and 1974), it became clear that part of the signal
53 reflected glacial-interglacial changes in continental ice volume and hence sea level variations.
54 The oxygen isotope composition of foraminiferal calcite ($\delta^{18}O_c$) is thus controlled by the
55 temperature of calcification (Urey, 1947; Epstein et al., 1953) but also by the oxygen isotope
56 composition of seawater ($\delta^{18}O_w$). The relative contribution of these two factors cannot be
57 deconvolved without an independent measure of the temperature at the time of calcification
58 such as e.g. Mg/Ca (e.g. Nürnberg et al., 1996; Rosenthal et al., 1997; Rathburn and DeDeckker,
59 1997; Hastings et al., 1998; Lea et al., 1999; Lear et al., 2002; Toyofuku et al., 2000; Anand et
60 al., 2003, al., Kisakurek et al., 2008; Duenas-Bohorquez et al., 2009, 2011; Honisch et al., 2013;
61 Kontakiotis et al., 2016; Jentzen et al., 2018). The sea surface temperature (SST) reconstructed
62 from Mg/Ca of foraminiferal calcite has, therefore, increasingly been used in combination with
63 the $\delta^{18}O$ signal measured on the same material, to estimate $\delta^{18}O_w$, global ice volume and to
64 infer past sea surface salinity (SSS) (e.g. Rohling 2000, Elderfield and Ganssen, 2000; Schmidt
65 et al., 2004; Weldeab et al., 2005; 2007). These studies also showed that, because of error
66 propagation, inaccuracies in the different proxies combined for the reconstruction of past sea
67 water $\delta^{18}O$ and salinity obstruct meaningful interpretations. Hence, while there is an
68 understandable desire to apply empirical proxy-relationships down-core, additional calibrations
69 appear necessary to make reconstructions more robust. Calibrations using foraminifera sampled
70 from surface seawater (0-10m deep), provide the best possibility to avoid most of the artefacts
71 usually seen when using specimen from core tops or culture experiments for calibration
72 purposes. Here, we report a calibration based on *Globigerinoides sacculifer*, which should now
73 and will be referenced in this manuscript as *Trilobatus sacculifer* (Spezzaferri et al., 2015),
74 from the Atlantic Ocean. Mg and Sr concentrations were measured on individual specimens
75 with Laser Ablation-Inductively Coupled Plasma-Mass Spectrometry (LA-ICP-MS), while the



76 oxygen isotope composition of the same tests as used for the elemental analyses was
77 subsequently measured by Isotope ratio Mass Spectrometry (IRMS). Environmental parameters
78 (temperature: T, salinity: S, dissolved inorganic carbon: DIC and alkalinity: ALK) but also the
79 isotopic composition (O_{18w}) of the seawater the foraminifers were growing in, were measured.
80 The primary objectives of this study are to test and improve the calibration of (1) both the
81 Mg/Ca and oxygen isotope paleothermometer for *T. sacculifer*, a paleoceanographically
82 relevant species; (2) evaluate the agreement between observed and predicted δ_{18O_w} and (3) test
83 potential for SSS reconstructions of the Atlantic Ocean. Our results indicate that the best
84 possible salinity reconstruction based on locally calibrated equations from the present study,
85 only allowed reconstruction with an uncertainty of ± 2.49 . Such an uncertainty does not allow
86 for viable (paleo)salinity data. This is subsequently confirmed by a Monte Carlo simulation,
87 applied to test successive reconstructions in an ‘ideal case’, where explanatory variables are
88 known. This simulation shows that from a pure statistical point of view, successive
89 reconstructions involving Mg/Ca and δ_{18O_c} preclude salinity reconstruction with a precision
90 better than ± 1.69 and hardly better than ± 2.65 , due to error propagation. Nevertheless, a direct
91 linear fit based on the same measured variables (Mg/Ca and $\delta^{18}O_c$), and leading to much better
92 estimation of salinity (± 0.26), could be established.

93

94

2. MATERIAL AND METHODS

95

2.1. Collection procedure

96
97 Foraminifera were collected between October and November 2005, on board of the research
98 vessel Polarstern (ANT XXIII/1) during a meridional transect of the Atlantic Ocean
99 (Bremerhaven/Germany - Cape Town/South of Africa; Fig. 1a). Foraminifera were
100 continuously collected from a depth of ca. 10 m using the ship’s membrane pump (3 m³/h). The
101 water flowed into a plankton net (125 μ m) that was fixed in a 1000 L plastic tank with an
102 overflow (Fig 1b). Every eight hours, the plankton accumulated in the net was collected.
103 Temperature and salinity of surface seawaters were continuously recorded by the ship’s
104 systems, and discrete water samples were collected for later analyses of total ALK, DIC and
105 δ_{18O_w} (see Tab. 1). Plankton and water samples were poisoned with buffered formaldehyde
106 solution (20%) and HgCl₂ (1.5 ml with 70gL⁻¹ HgCl₂ for 1 L samples), respectively. In total,
107 more than seventy plankton samples were collected during the transect, covering a large range
108 in both temperature and salinity. Specimens of *T. sacculifer* from thirteen selected stations,
109 selected as to maximize temperature and salinity ranges, were picked and prepared for analyses.



110 Salinity, temperature, DIC, ALK and $\delta_{18}\text{O}_w$ data reported in this paper represent
111 October/November values for the selected stations.

112

113 **2.2. Description of species**

114 *Trilobatus sacculifer* is a spinose species with endosymbiotic dinoflagellates inhabiting the
115 shallow (0-80 m deep) tropical and subtropical regions of the world oceans. This species
116 displays a large tolerance to temperature (14-32°C) and salinity (24-47) (Hemleben et al., 1989;
117 Bijma et al., 1990). Based on differences in the shape of the last chamber of adult specimens,
118 various morphotypes can be distinguished. Among others the last chamber can be smaller than
119 the penultimate chamber, in which case it is called kummerform (kf). This species shows an
120 ontogenetic depth migration and predominantly reproduces at depth around full moon (Bijma
121 and Hemleben, 1993). Just prior to reproduction a secondary calcite layer, called gametogenic
122 (GAM) calcite is added (Bé et al., 1982; Bijma and Hemleben, 1993; Bijma et al., 1994).
123 Juveniles (<100µm) ascend in the water column and reach the surface after less than
124 approximately 2 weeks. Pre-adult stages then slowly descend within 9-10 days to the
125 reproductive depth. In our samples (collected between 0 and 10 m depth), *T. sacculifer*
126 specimens have not yet added the Mg-enriched gametogenic calcite, which generally occurs
127 deeper in the water column just prior to reproduction. Therefore, only the trilobus morphotype
128 without GAM calcite is considered (230µm to 500µm) in this study, which limits the
129 environmental, ontogenetic and physiological variability between samples and should be taken
130 into account when compared to other calibrations based on core top and/or sediment trap
131 collected specimens.

132

133 **2.3. Seawater analysis**

134 The DIC and ALK analyses of the sea water were carried out at the Leibniz Institute of Marine
135 Sciences at the Christian-Albrechts University of Kiel, (IFM-GEOMAR), Germany. Analyses
136 were performed by extraction and subsequent coulometric titration of evolved CO₂ for DIC
137 (Johnson et al., 1993), and by open-cell potentiometric seawater titration for ALK (Mintrop et
138 al., 2000). Precision / accuracy of DIC and ALK measurements are 1 µmol kg⁻¹ / 2 µmol kg⁻¹
139 and 1.5 µmol kg⁻¹ / 3 µmol kg⁻¹, respectively. Accuracy of both DIC and ALK was assured by
140 the analyses of certified reference material (CRM) provided by Andrew Dickson from Scripps
141 Institution of Oceanography, La Jolla, USA. Measurements of $\delta_{18}\text{O}_w$ were carried out at the
142 Faculty of Geosciences, Utrecht University, Netherlands. Samples were measured using a
143 GasBench II - Delta plus XP combination. Results were corrected for drift with an in-house



144 standard (RMW) and are reported on V-SMOW scale, with a precision of 0.1‰ and accuracy
145 verified against NBS 19 of 0.2‰ respectively. For reconstruction calculations $\delta_{18}\text{Ow}$ data were
146 corrected to the PDB scale by subtracting 0.27‰ (Hut, 1987).

147

148 **2.4. Carbonate analysis**

149 2.4.1. Foraminiferal sample preparation

150 Under a binocular microscope, maximum test diameter of each specimen was measured and
151 individual tests were weighed on a microbalance (METTLER TOLEDO, precision $\pm 0.1\mu\text{g}$).
152 Since the foraminifera were never in contact with sediments, the rigorous cleaning procedure
153 required for specimens collected from sediment cores, was not necessary. Prior to analysis the
154 tests were cleaned following a simplified cleaning procedure: All specimens were soaked for
155 30 min in a 3-7% NaOCl solution (Gaffey and Brönniman, 1993). A stereomicroscope was used
156 during cleaning and specimens were removed from the reagent directly after complete
157 bleaching. The samples were immediately and thoroughly rinsed with deionised water to ensure
158 complete removal of the reagent. After cleaning, specimens were inspected with scanning
159 electron microscopy and showed no visible signs of dissolution. This cleaning procedure
160 preserves original shell thickness and thus maximises data acquisition during laser ablation.
161 Foraminifera were fixed on a double-sided adhesive tape and mounted on plastic stubs for LA-
162 ICP-MS analyses.

163

164 2.4.2. Elemental composition analysis

165 For each station, 5–8 specimens were analysed. Their last chambers were ablated using an
166 Excimer 193 nm deep ultraviolet laser (Lambda Physik) with GeoLas 200Q optics (Reichert et
167 al, 2003) creating 80 μm diameter craters. Pulse repetition rate was set at 6 Hz, with an energy
168 density at the sample surface of 1 J/cm². The ablated material was transported on a continuous
169 helium flow into the argon plasma of a quadrupole ICP-MS instrument (Micromass Platform)
170 and analysed with respect to time. Ablation of calcite requires ultraviolet wavelengths as an
171 uncontrolled disruption would result from higher wavelengths. By using a collision and reaction
172 cell spectral interferences on the minor isotopes of Ca (⁴²Ca, ⁴³Ca and ⁴⁴Ca) were reduced and
173 interferences of clusters like ¹²C¹⁶O¹⁶O were prevented. Analyses were calibrated against NIST
174 (U.S. National Institute of Standards and Technology) 610 glass using the concentration data
175 of Jochum et al. (2011) with Ca as internal standard. For Ca quantification, mass 44 was used
176 while monitoring masses 42 and 43 as internal check. In the calcite, the Ca concentration was
177 set at 40%, allowing direct comparison to trace metal/Ca from traditional wet-chemical studies.



178 Mg concentrations were calculated using masses 24 and 26; Sr concentrations were calculated
179 with mass 88. One big advantage in using LA-ICP-MS measurements is that single laser pulses
180 remove only a few nanometers of material, which allows high resolution trace elements profiles
181 to be acquired (e.g. Reichart et al., 2003; Regenberg et al., 2006; Dueñas-Bohórquez et al.,
182 2009, 2010, Hathorne et al., 2009; Munsel et al., 2010; Dissard et al., 2009; 2010a and b; Evans
183 et al., 2013; 2015; Steinhardt 2014, 2015; Fehrenbacher et al., 2015; Langer et al., 2016; Koho
184 et al., 2015; 2017; Fontanier et al., 2017; De Nooijer et al., 2007, 2014, 2017a and b; Jentzen et
185 al., 2018, Schmitt et al., 2019; Levi et al., 2019). Element concentrations were calculated for
186 the individual ablation profiles integrating the different isotopes (glitter software). Even though
187 the use of a single or very few specimens, can be criticised when determining foraminifera
188 Mg/Ca and $\delta_{18}\text{O}$ in order to perform paleoclimate reconstructions instead of more traditional
189 measurements, Groeneveld et al., (2019) recently demonstrated that for both proxies, single
190 specimen variability is dominated by seawater temperatures during calcification, even if the
191 presence of an ecological effect leading to site-specific seasonal and depth habitat changes is
192 also noticeable.

193

194 **2.5. Stable isotope analysis**

195 The specimens used for elemental composition analyses using LA-ICP-MS were subsequently
196 carefully removed from the plastic stubs and rinsed with deionised water before measuring their
197 stable isotope composition. Depending on shell weight, 2 to 3 foraminifera were necessary to
198 obtain a minimum of 20 μg of material, required for each analysis. Analyses were carried out in
199 duplicate for each station. The results, compiled in table 2, represent average measurements.
200 The analyses were carried out at the Department of Earth Sciences of Utrecht University (The
201 Netherlands), using a Kiel-III -Finnigan MAT-253 mass spectrometer combination. The $\delta_{18}\text{O}_\text{c}$
202 results are reported in ‰ PDB. Calibration was made with NBS-19 (precision of 0.06-0.08 ‰
203 for sample size 20-100 μg , accuracy better than 0.2‰).

204

205 **2.6. Statistical analysis**

206 Within this manuscript, all statistical analyses with regards to elemental and isotopic data, were
207 carried out using the program R with default values (R Development Core Team (2019)).

208

209

209 **3. RESULTS**

210

211 **3.1. Elemental composition**



212 Overall values of the Mg/Ca and Sr/Ca ratios in the tests of *T. sacculifer* varied from 1.78 to
213 5.86 mmol/mol (Fig. 2a) and 1.41 to 1.52 mmol/mol (fig. 2b), respectively (Tab. 2). These
214 Mg/Ca concentrations compare well with results found in literature for this species from either
215 culture experiments, plankton tow, or surface sediment, growing at the same temperatures (e.g.
216 Nürnberg et al., 1996; Anand et al. 2003, Regenberg et al., 2009, Fig. 3). Similarly, the overall
217 variation in Sr/Ca-values reported in this study is comparable to that observed in core top and
218 cultured *G. ruber* and *T. sacculifer* combined, for comparable salinity and temperature
219 conditions, (varying between 1.27 to 1.51mmol/mol; e.g. Cleroux et al., 2008; Kisakürek et al.,
220 2008; Dueñas-Bohórquez et al., 2009).

221
222
223

224 The relationship between measured temperatures and both Mg/Ca and Sr/Ca ratios were
225 calculated using least square differences. Both show a good correlation with surface water
226 temperature (Fig. 2, Tab. 3). The Mg/Ca ratio increases exponentially by 8.3%/°C (best fit)
227 (Mg/Ca and Sr/Ca ratios given in mmol/mol):

$$228 \text{Mg/Ca} = (0.42 \pm 0.13) \exp((0.083 \pm 0.001) * T [^{\circ}\text{C}]), R^2 = 0.86 \quad \text{pvalue} = 2.9 \times 10^{-6} \quad (\text{equation 1})$$

229

230 whereas Sr/Ca ratio increases linearly by 0.6%/°C (Fig. 2a and b), best fit:

231

$$232 \text{Sr/Ca} = (0.009 \pm 0.002) * T + (1.24 \pm 0.05), R^2 = 0.67 \quad \text{pvalue} = 5 \times 10^{-4} \quad (\text{equation 2})$$

233

234 Combining Mg and Sr data for a non-linear multivariate regression allows improvement of the
235 correlation with temperature, best fit:

236

237

$$238 T = -(27 \pm 15) + (8 \pm 1) * \ln(\text{Mg/Ca}) + (28 \pm 11) * \text{Sr/Ca}, \text{pvalue Mg/Ca: } 2.10^{-4} \quad (\text{equation 3})$$

239

$$R^2 = 0.92 \quad \text{pvalue} = 2 \times 10^{-4}$$

240

241 Regression for the relationship between salinity and Mg/Ca ratios does not show any clear
242 correlation ($R^2 = 0.09$, p-value = 0.32). This is in good agreement with previous culture
243 experiments studies which only report a minor sensitivity of Mg/Ca to salinity in planktonic
244 foraminifera (e.g. Dueñas-Bohórquez et al., 2009; Hönisch et al., 2013; Kisakürek et al., 2008;
245 Nürnberg et al., 1996). The correlation observed between Sr/Ca ratios and salinity ($R^2 = 0.29$, p-



246 value=0.053) is better compared to that between Mg/Ca and salinity, but remains relatively
247 weak. Nevertheless, recalculated regressions of Mg/Ca, incorporating salinity, show an
248 improvement of the correlation with temperature, best fit:

249

$$250 \quad \ln(\text{Mg/Ca}[\text{mmol/mol}]) = (-5.02 \pm 2) + (0.09 \pm 0.009) * T + (0.11 \pm 0.05) * S,$$

$$251 \quad R^2 = 0.91 \quad p\text{value} = 5e-06$$

252

253 This result is in good agreement with the recent study of Gray and Evans (2019), who reported
254 the minor Mg/Ca sensitivity of *Trilobatus sacculifer* to salinity ($3.6 \pm 0.01\%$ increase per
255 salinity unit) and described, based on previously published culture experiments' data (Dueñas-
256 Bohórquez et al., 2009; Hönisch et al., 2013; Kisakürek et al., 2008; Lea et al., 1999; Nürnberg
257 et al., 1996), a similar fit allowing to assess the sensitivity of foraminiferal Mg/Ca of *T.*
258 *sacculifer* to temperature and salinity combined.

$$259 \quad \text{Mg/Ca} = \exp(0.054(S-35) + 0.062T - 0.24) \quad \text{RSE: 0.51} \quad \text{Gray and Evans (2019)}$$

260 In order to compare both equations, Mg/Ca values from our study were used to reconstruct
261 temperature and salinity using the fit established per Gray and Evans (2019), versus
262 reconstructed temperature and salinity using our fit. The observed R^2 are then 0.99 and 0.48 for
263 temperature and salinity, respectively. We can conclude, that if the equation of Evans and Gray
264 is in perfect agreement with our equation with regards to the temperature parameter, this is not
265 the case for salinity, which shows a strong difference between the two equations, most probably
266 explained by the weak correlation of Mg/Ca to salinity.

267 3.2. Stable isotopes concentration

268 The $\delta_{18}\text{O}$ (PDB) values of the tests ($\delta_{18}\text{Oc}$) and of the seawater ($\delta_{18}\text{Ow}$) vary from -0.70 to -
269 2.98‰ and from 0.74 to 1.25‰, respectively (Tab. 1 and 2). The relationship between
270 temperature and the foraminiferal $\delta_{18}\text{O}$ (expressed as a difference to the $\delta_{18}\text{Ow}$ of the ambient
271 seawater) was estimated with a linear least squares regression:

272

$$273 \quad T = (11.82 \pm 1.3) - (4.82 \pm 0.45) * (\delta_{18}\text{Oc} - \delta_{18}\text{Ow}) [\text{‰}]; R^2 = 0.90 \quad (\text{equation 4})$$

274

275 The oxygen isotope fractionation ($\delta_{18}\text{Oc} - \delta_{18}\text{Ow}$) shows a strong correlation with *in situ* surface
276 water temperature (linear increase of $0.17\text{‰}/^\circ\text{C}$).

277



278 **3.3. Comparison with previously established *T. sacculifer* temperature reconstruction**
279 **equations**

280 As mentioned above, average juvenile and pre-adult *T. sacculifer* specimen only spend between
281 9 to 10 days in surface waters. Therefore, measured *in situ* temperature is representative of the
282 calcification temperatures. This is supported by the strong correlation between measured
283 temperature and $\delta_{18}\text{O}$ analyses ($R_2=0.90$, equation 4), and measured temperature vs. Mg/Ca,
284 ($R_2=0.87$, equation 1). Nevertheless, diurnal variations in temperatures cannot be discarded and
285 may induce a slight offset between measured average temperature and mean calcification
286 temperature.

287

288 For comparison, three Mg/Ca temperature calibrations for *T. sacculifer* were considered in this
289 manuscript. The equation of Nürnberg et al. (1996) based on laboratory cultures, (2) the
290 equation established by Anand et al. (2003) based on sediment trap samples and (3) the equation
291 derived by Regenberg et al. (2009) based on surface sediment samples of the Tropical Atlantic
292 Ocean. In each of these studies only *T. sacculifer* without SAC chamber were considered, (Tab.
293 3).

294 Similarly, in addition to equation 4 established in this study, three $\delta_{18}\text{O}$ based paleo-temperature
295 equations for *T. sacculifer* were used for comparison with our data set: (1) Erez and Luz, (1983)
296 and, (2) Spero et al. (2003), both based on cultured specimens, and (3) Mulitza et al. (2003)
297 based on surface water samples (Fig. 4; Tab. 3).

298

299 **3.4. Correlation between measured $\delta_{18}\text{O}$ /Salinity**

300 Salinity and the oxygen isotope composition of surface seawater were measured for 23 stations
301 located between 33°N and 27°S of the Eastern Atlantic Ocean (Tab. 4), including the thirteen
302 stations represented in figure 1, where foraminifera were sampled. The $\delta_{18}\text{O}_w$ -salinity
303 relationship (equation 5) is plotted in figure 5.

304

305
$$\delta_{18}\text{O}_w = (0.194 \pm 0.04) * S - (5.8 \pm 1.5), R^2=0.53 \quad (\text{equation 5})$$

306

307 For comparison, the $\delta_{18}\text{O}_w$ -salinity relationship for the tropical Atlantic Ocean calculated by
308 Paul et al. (1999) (from 25°S to 25°N) based on GEOSECS data, and by Regenberg et al.
309 (2009), based on data from Schmidt 1999 (30°N–30°S), are plotted in the same figure.
310 Temporal, geographical and depth differences in sampling, as well as analytical noise, are most
311 probably responsible for the observed variations.



312

313

4. DISCUSSION

314 4.1. Intra-test variability

315 The Mg/Ca and Sr/Ca composition of foraminiferal calcium carbonate was determined using
316 laser ablation ICP-MS of the final (F) chamber of size-selected specimen. Eggins et al., (2003)
317 report that the Mg/Ca composition of sequentially precipitated chambers of different species
318 (including *T. sacculifer*) are consistent with temperature changes following habitat migration
319 towards adult life-cycle stages. As described for *T. sacculifer* in the Red Sea (Bijma and
320 Hemleben, 1994), juvenile specimens (<100µm) migrate to the surface, where they stay about
321 9-10 days, before descending to the reproductive depth (80m). The addition of GAM calcite
322 proceeds immediately prior to gamete release (Hamilton et al., 2008). The specimens
323 considered in this study were collected between 0 and 10 meters depth, and GAM calcite was
324 not detected. This limits the impact of variability due to migration, reduces potential ontogenic
325 vital effects responsible for inter-chamber elemental variations (Dueñas-Bohórquez, 2010) and,
326 avoids variability due to variable amounts of GAM calcite precipitated (Nürnberg et al., 1996).
327 This is confirmed by the strong correlation ($R^2=0.87$) observed between our Mg/Ca-
328 reconstructed temperature vs. measured surface temperature. In agreement with measurements
329 on specimens from culture experiments (Dueñas-Bohórquez, 2009), Mg-rich external surfaces
330 (GAM calcite) were not observed in our samples.

331 Because the diameter of the laser beam used in this study was 80µm, it represents a reliable
332 mean value of elemental concentration of the last chamber wall, for every analysis of a single
333 shell a full ablation of the wall chamber was performed (until perforation was completed). For
334 comparison, results from traditional ICP-OES Mg/Ca analyses (Regenberg et al., 2009),
335 electron microprobe (Nürnberg et al., 1996) and laser ablation ICP-MS (this study) are plotted
336 in figure 3a and suggest comparable foraminiferal Mg/Ca ratios for *T. sacculifer* at similar
337 temperatures.

338

339 4.2. Incorporation of Sr into Mg/Ca-Temperature calibrations

340 Combining Mg and Sr data to compute temperature was first suggested by Reichart et al. (2003)
341 for the aragonitic species *Hoeglundina elegans*. It has been demonstrated that variables other
342 than temperature, such as salinity and carbonate chemistry (possibly via their impact on growth
343 rate) are factors influencing Sr incorporation into calcite (e.g. Lea et al., 1999, Dueñas-
344 Bohórquez et al., 2009; Dissard et al., 2010a; Dissard et al., 2010b). The good correlation of
345 Sr/Ca with temperature in our results ($R^2=0.67$, p value= 5.e-04, Fig 2b), also suggests that



346 temperature exerts a major control on the amount of Sr incorporated into *T. sacculifer*' tests.
347 However, Sr/Ca concentration also shows a correlation with salinity ($R^2=0.29$, p -value=0.053),
348 which is not observed for Mg ($R^2=0.09$, p -value=0.32). Therefore, the incorporation of Sr into
349 the Mg-T reconstruction equation might improve temperature reconstruction by accounting for
350 the impact of salinity. It has recently been suggested that the Sr incorporation in benthic
351 foraminiferal tests is affected by their Mg contents (Mewes et al., 2015; Langer et al.; 2016).
352 However, as pointed out in Mewes et al., (2015), calcite's Mg/Ca needs to be over 30-50mmol
353 in order to noticeably affect Sr partitioning. There is no obvious reason to assume that
354 planktonic foraminifera should have a different Mg/Ca threshold. Therefore, with a
355 concentration between 2 to 6 mmol/mol (Sadekov et al., 2009), the observed variation in Sr
356 concentration in *T. sacculifer*' tests can be safely considered to be independent of the Mg/Ca
357 concentrations. Hence, other environmental parameters such as temperature, salinity and/or
358 carbonate chemistry, potentially via an impact on calcification rates, must control Sr/Ca values.
359

360 The standard deviation of measured temperatures versus reconstructed temperature was
361 calculated for each of the three Mg-temperature equations established in this study. For
362 equation (1), based on Mg/Ca only, $SD=1.37$, for equation (3), based on both Mg/Ca and Sr/Ca,
363 $SD=0.98$, and for equation (4), based on Mg/Ca ratio and salinity, $SD=1.03$. Incorporation of
364 Sr into the Mg-Temperature reconstruction equation resulted in the standard deviation the
365 closest to 1 ($SD=0.98$), indicating that this statistically improved reconstructions possibly by
366 attenuating the salinity effect as well as potentially other environmental parameters such as
367 variations in carbonate chemistry or the effect of temperature itself. Therefore, the combination
368 of Mg/Ca and Sr/Ca should be considered to improve temperature reconstructions (Tab. 3). For
369 the remainder of this discussion, and in order to compare our data with previously established
370 calibrations for *T. sacculifer*, the equation based on Mg/Ca alone (equation 1) will be
371 considered.

372

373 **4.3 Comparison with previous *T. sacculifer* Mg/Ca-Temperature calibrations.**

374 Mg/Ca ratios measured on *T. sacculifer* from our study show a strong correlation with measured
375 surface water temperature ($R^2=0.86$, p value= $2.9e-06$) (Fig. 2a), increasing exponentially by
376 8.3% per °C. The relation with temperature (equation 1) is comparable to the one published by
377 Nürnberg et al., (1996) and within the standard error of the calibration (Fig. 3a). This implies
378 that the temperature controlled-Mg incorporation into *T. sacculifer* tests is similar under culture
379 conditions as it is in natural surface waters. The equation established by Duenas-Bohorquez et



380 al., (2010) based on *T. sacculifer* specimen from culture experiments integrates ontogenetic
381 (chamber stage) effects. Even though incorporating the ontogenetic impact may improve
382 temperature reconstructions based on Mg/Ca ratios, this is not routinely done for paleo-
383 temperature reconstruction using *T. sacculifer*. Therefore, the equation of Nürnberg et al.,
384 (1996) is used in our study for comparison of various reconstruction scenarios.

385 A comparable regression (similar slope) has been established for *T. sacculifer* from tropical
386 Atlantic and Caribbean surface sediment samples by Regenberg et al. (2009) (Fig 3a). This
387 regression predicts Mg concentrations that are about 0.15 mmol/mol higher compared to our
388 study. Because the Mg-T calibration from Regenberg et al. (2009) is based on sediment-surface
389 samples, Mg concentrations were correlated with reconstructed mean annual temperatures. This
390 potentially leads to an over or under-estimation of temperatures depending on the seasonality
391 of the growth period and might explain the observed difference between the two regressions.
392 Due to sample limitation, we analysed foraminifera from a wider size fraction (230µm to
393 500µm), compared to Regenberg et al. (2009) (355-400µm), introducing an additional bias
394 between the two datasets (Duenas-Bohorquez et al., 2010; Friedrich et al., 2012). Finally,
395 Regenberg et al. (2009), compiled data of samples from the tropical Atlantic and Caribbean
396 Ocean, while we collected samples from the Eastern tropical Atlantic. All of these potential
397 biases can easily explain the small discrepancy observed between our regression and the one
398 from Regenberg et al., (2009). Interestingly, Jentzen et al., (2018), were able to compare Mg/Ca
399 ratios measured on *T. sacculifer* from both surface sediment samples of the Caribbean sea and
400 specimen sampled with a plankton net nearby. They observed a similar systematic increased
401 Mg/Ca ratio in fossils tests of *T. sacculifer* (+0.7 mmol/mol-1) compared to living specimens,
402 arguing that different seasonal signals were responsible for the observed difference. However,
403 it is interesting to note that the Mg/Ca differences observed between living *T. sacculifer* (e.g.
404 this study and Jentzen et al., 2018) and fossils specimens (e.g. Regenberg et al., 2009 and
405 Jentzen et al., 2018) could also be explained by the presence of GAM calcite on *T. sacculifer*
406 from sediment samples, as GAM calcite is enriched with Mg compared to pre-gametogenetic
407 calcite precipitated at the same temperature (Nurnberg et al., 1996). If Jentzen et al., (2018) and
408 Regenberg et al. (2009) do not describe the presence or absence of GAM calcite on *T. sacculifer*
409 specimens analysed in their studies, a study on the population dynamics of *T. sacculifer* from
410 the central Red Sea Bijma and Hemleben (1990) concluded that the rate of gametogenesis
411 increased exponentially between 300 and 400µm to reach a maximum of more than 80% at
412 355µm (sieve size =500µm real test length). It can therefore safely be assumed that the Mg/Ca



413 difference between living specimens from the plankton and empty shells from the sediment is
414 due to GAM calcite.

415 The Mg-Temp data obtained by Jentzen et al., (2018) is however, in good agreement with the
416 equation established by Regenberg et al., (2009), and will therefore not be considered separately
417 in this study. The overall strong similarity observed between our regression and the one from
418 Regenberg et al. (2009), indicates nevertheless that Mg-temp calibrations established on *T.*
419 *sacculifer* specimen from plankton tow, can be applied to *T. sacculifer* (without Sac) from the
420 surface-sediment, even if these applications have to be considered with care and only on
421 sediment samples showing no sign of dissolution.

422 In contrast, the equation of Anand et al., (2003) based on sediment trap samples, is appreciably
423 different (Fig. 3b). This may be due to: (1) difference in cleaning and analytical procedures, (2)
424 uncertainty in estimated temperature (3) addition of GAM calcite at greater depth. Anand et al.,
425 (2003) fixed the intercept of the exponential regression for *T. sacculifer* to the value obtained
426 for a multispecies regression and subsequently recalculated for each species the pre-exponential
427 coefficients. Using this approach their new equation for *T. sacculifer* is: $Mg/Ca = 0.35 \exp(0.09 * T)$,
428 which is identical to Nürnberg et al., (1996) and equation 1 from our study. Still, this
429 implicitly assumes a common temperature dependence exists for all species, which is not
430 realistic. To avoid *a priori* assumptions only the primary equation of Anand et al., (2003) (see
431 Tab. 3) is considered in this study.

432

433 **4.4. Comparison with previous $\delta^{18}O$ -Temperature calibrations.**

434 As for Mg/Ca, the oxygen isotope composition also shows a strong correlation with measured
435 surface water temperature ($R^2=0.90$). The *T. sacculifer* $\delta^{18}O$ -temperature equation of Spero et
436 al., (2003), based on a culture experiment, is very similar to equation 4 in our study. However,
437 sensitivity (slope) differs within the uncertainties calculated for equation 4. As no uncertainties
438 are given for the Spero et al., (2003) equation, it is difficult to determine whether these
439 equations are statistically different or not. In contrast, the equation of Mulitza et al., (2003), has
440 a similar slope (within uncertainties) but a higher intercept (Fig. 4a). The equation of Erez and
441 Luz, (1983) differs considerably from equation 4, for both slope and intercept parameters.
442 Bemis et al., (1998) suggested a bias in the calibration due to uncontrolled carbonate chemistry
443 during the experiments of Erez and Luz (1983) (a decrease in pH, e.g. due to bacterial growth
444 in the culture medium or to a higher CO_2 concentration in the lab (air conditioners, numerous
445 people working in the same room etc), would quickly lead to an increase in $\delta^{18}O$ of culture-
446 grown foraminifera). This could explain the observed effect between our study (equation 4) and



447 the calibration from Erez and Luz (1983). Although the equation of Mulitza et al., (2003) is
448 also based on *T. sacculifer* collected from surface waters, their equation is significantly different
449 from equation (4). This deviation could possibly be due to a difference in size fractions
450 considered in the two studies (230 to 500 μm , and 150 to 700 μm for this study and Mulitza et
451 al., (2003), respectively). Berger et al. (1979), already reported that large *T. sacculifer* tests are
452 enriched in $\delta_{18}\text{O}$ relative to smaller ones (variation of 0.5‰ between 177 and 590 μm).
453 Similarly, in culture experiments, larger shells of *Globigerina bulloides* are isotopically heavier
454 relative to smaller specimens (variation of approximately 0.3‰ between 300 to 415 μm ,
455 Bemis et al., 1998). Jentzen et al., (2018) reported that: ‘Enrichment of the heavier ^{18}O isotope
456 in living specimens below the mixed layer and in fossil tests is clearly related to lowered in situ
457 temperatures and gametogenic calcification’. Gametogenic calcite has been shown to enrich
458 $\delta_{18}\text{O}$ signatures by about 1.0-1.4‰ relative to pregametogenic *T. sacculifer* (Wyceh et al.,
459 2018). Finally, variation in light intensity (e.g. due to different sampling period and/or sampling
460 location), may have influenced the $\delta_{18}\text{O}$ composition via an impact on symbiont activity (Spero
461 and DeNiro, 1987). Bemis et al. (1998) demonstrated that in seawater with ambient $[\text{CO}_2]$,
462 *Orbulina universa* shells grown under high light level ($> 380 \mu\text{Einst m}^{-2} \text{s}^{-1}$) are depleted in O_{18}
463 by on average 0.33‰ relative to specimens grown under low light levels (20-30 $\mu\text{Einst m}^{-2} \text{s}^{-1}$).
464 The different correlation between $\delta_{18}\text{O}$ and temperature reported by Mulitza et al., (2003)
465 may be caused by size fraction differences, different sampling time, light intensity, differences
466 in calcification depth or hydrography, or a combination of factors. These are all potential biases
467 that could explain the steeper intercept observed by Mulitza et al., (2003) relative to our study.
468

469 **5. Reconstructions**

470 A few scenarios are considered in the following section, in which one, two or three proxy
471 equations are combined to solve for salinity.

472

473 Three Mg/Ca-paleo-temperature equations (Nürnberg et al., 1996; Regenberg et al., 2009; and
474 Anand et al., 2003) were used to compare “reconstructed” temperatures to the known *in situ*
475 surface waters temperatures. The mean foraminiferal Mg/Ca ratio measured at each of our
476 stations was inserted into each of the three equation and solved for temperature (Fig. 3b.). The
477 linear regression of reconstructed temperatures based on Nürnberg et al. (1996) overlaps almost
478 perfectly with the theoretical best fit. This confirms that calibrations based on culture
479 experiments (the primary geochemical signal recorded in the tests) are very well-suited for
480 reconstructing surface water temperature. The regression from Regenberg et al., (2009)



481 reconstructed surface temperature that are too warm. This is in agreement with the fact that the
482 Mg/Ca ratio from surface sediment foraminifera are slightly higher than for living specimen
483 (Jentzen et al. 2018). The offset increases with decreasing temperature (0.5°C and 1.5°C
484 respectively at 30°C and 16°C). Finally, the reconstructed temperature using the equation from
485 Anand et al. (2003), shows a strong systematic offset. Because the equation of Nürnberg et al.,
486 (1996) matched our measured temperatures almost perfectly, their equation will be used to
487 analyse further reconstruction. Still, we acknowledge that downcore reconstructions will
488 inevitably also involve GAM calcite and hence other calibrations established using specimens
489 collected deeper in the water column or in the sediment should be better suitable. Similarly,
490 three $\delta_{18}\text{O}$ -paleo temperature equations (Erez and Luz, 1983; Mulitza et al., 2003; Spero et al.,
491 2003) were tested to reconstruct $\delta_{18}\text{Oc}$ - $\delta_{18}\text{Ow}$. The equation of Erez and Luz, (1983), shows a
492 significant systematic overestimation of $\delta_{18}\text{Oc}$ - $\delta_{18}\text{Ow}$, and will therefore not be considered any
493 further. Measured surface water temperatures at our 13 stations were inserted into the equations
494 of Mulitza et al., (2003) and Spero et al., (2003) to derive $\delta_{18}\text{Oc}$ - $\delta_{18}\text{Ow}$ (Fig. 4). The $\delta_{18}\text{Oc}$ -
495 $\delta_{18}\text{Ow}$ reconstructions based on the equation of Mulitza et al. (2003) and Spero et al. (2003),
496 are both slightly more positive, than the theoretical best fit. In order to test the robustness of
497 $\delta_{18}\text{Ow}$ reconstructions from paleoceanographic literature (e.g. Nürnberg and Groeneveld, 2006;
498 Bahr et al., 2011), we use the reconstructed temperatures based on the Mg/Ca-paleo-
499 temperature equation from Nürnberg et al., (1996) to predict $\delta_{18}\text{Ow}$ using measured $\delta_{18}\text{Oc}$ and
500 the equations from Mulitza et al., (2003) and Spero et al. (2003). The reconstructed $\delta_{18}\text{Oc}$ -
501 $\delta_{18}\text{Ow}$ from inserting the Mg/Ca temperature into these equations is slightly overestimated
502 (0.5‰), but the offsets remain small enough to consider these as reasonable reconstructions.

503

504 Nevertheless, when reconstructing $\delta_{18}\text{Ow}$ by inserting the Mg/Ca temperature and measured
505 $\delta_{18}\text{Oc}$ in both equations, the correlation coefficients of the linear regressions are weak ($R^2 =$
506 0.19 and 0.13 for Spero et al., 2003 and Mulitza et al., 2003, respectively) demonstrating that
507 the reconstructed $\delta_{18}\text{Ow}$ is not very reliable, therefore no reconstruction of salinity using these
508 equations will be further tested in this manuscript.

509

510 Nevertheless, to test the robustness of theoretical and empirical salinity reconstructions, we
511 have the perfect data set at hand, as every parameter is known from *in situ* measurement or
512 sampling. We will use the equations 1, 4 and 5 established in this study and presented in table
513 3, for demonstration purposes.

514



515
$$\text{Mg/Ca} = ae^{bT} \quad \text{Eq. 1}$$

516 with $a=0.42(\pm 0.13)$ and $b=0.083(\pm 0.001)$

517

518
$$T = c + d(\delta^{18}\text{O}_c - \delta^{18}\text{O}_w) \quad \text{Eq. 4}$$

519 with $c=12.08(\pm 1.46)$ and $d=-4.73(\pm 0.51)$

520

521
$$\delta^{18}\text{O}_w = eS + f \quad \text{Eq. 5}$$

522 with $e=0.171(\pm 0.04)$ and $f=-4.93(\pm 1.66)$

523 Classically, from those equations it is possible to extract variables estimated from the
524 observation Mg/Ca and $\delta^{18}\text{O}_c$ through the equations:

525
$$\hat{T} = \frac{1}{b}(\log(\text{Mg/Ca}) - \log(a)) \quad \text{Eq. 1'}$$

526
$$\widehat{\delta^{18}\text{O}_w} = \delta^{18}\text{O}_c - \frac{1}{d}(\hat{T} - c) \quad \text{Eq. 4'}$$

527
$$\hat{S} = \frac{1}{e}(\widehat{\delta^{18}\text{O}_w} - f) \quad \text{Eq. 5'}$$

528

529

530 Given that \hat{T} is estimated from the fit from Eq. 1' (fig. 3a) and $\widehat{\delta^{18}\text{O}_w}$ is estimated from Eq. 4',
531 \hat{S} is finally calculated from Eq. 5' (figure 5). Hence, the error in \hat{S} is an accumulation of errors
532 from successive fits. In this study the standard deviation of the fit between \hat{S} and the measured
533 salinity for the 13 stations is ± 2.49 and the R^2 is 0.33 (p-value 0.04) (Fig. 6a and b). In
534 conclusion, even the best possible salinity reconstruction based on locally calibrated equations
535 1, 4 and 5 from the present study only allows salinity reconstructions with a precision of ± 2.49 .
536 In the modern Atlantic Ocean, and based on recent sea surface salinity estimation (Vinogradova
537 et al., 2019), such a variability would not allow to distinguish water masses between 60°N to
538 60°S . Similarly, on a temporal timescale, given the regional salinity variations expected in most
539 of the ocean over glacial-interglacial cycles is less than $\pm 1, 2\sigma$ (Gray and Evans, 2019), such an
540 incertitude on salinity reconstruction would not even allow to distinguish modern *versus* last
541 glacial maximum water masses.

542

543 In the following steps, we quantify the error propagation more precisely. In simple cases, error
544 accumulation in an equation can be assessed by calculating the partial derivatives and by
545 propagating the uncertainties of the equation with respect to the predictors (Clifford, 1973).
546 However, for complex functions the calculation of partial derivatives can be tedious. Here, error



547 propagation related to \hat{S} was computed by a Monte Carlo simulation, which is simple to
548 implement (Anderson, 1976). It is important to note that the propagated error with a
549 reconstructed salinity is a combination of fitting errors and errors associated with measurement
550 inaccuracies (Mg/Ca and $\delta^{18}\text{O}_c$). First, we will only consider the error related to the fitting
551 procedure, (Eq. 1', 4' and 5', assuming that variables (i.e. the data) are perfectly known without
552 uncertainties). For example, the fitting error related to Eq. 4' is computed by fitting $\delta^{18}\text{O}_w$
553 from measured $\delta^{18}\text{O}_c$ and measured Temperature, i.e. the data are known and not
554 approximated. This is done by adding random Gaussian noise, with standard deviation
555 corresponding to the RMSE (Root Mean Square error) of each fit (respectively 1.32°C for
556 Eq.1', 0.15‰ for Eq. 4' and 0.55 for Eq. 5'). The resulting standard deviation error for the
557 reconstructed Salinity based on 10000 fits following the Monte-Carlo approach amounted to
558 ± 1.69 (each fit using sampling from random distributions defined above). Hence, ± 1.69 is the
559 smallest possible error for salinity reconstructions, using the three steps above, only due to its
560 mathematics. We can also estimate the error propagation at each step: $\hat{T} \pm 1.32^\circ\text{C}$ (Eq.1'),
561 $\widehat{\delta^{18}\text{O}_w} \pm 0.45\%$ (Eq.4') and $\hat{S} \pm 1.69$ (Eq.5'). Now we will include the uncertainties related to
562 estimating the variables using proxy data. Hereto, some Gaussian noises simulating the
563 uncertainties of measured variables (Mg/Ca and $\delta^{18}\text{O}_c$) were introduced with standard
564 deviations taken from Table 2. The resulting standard deviation error increased to ± 2.65 .
565 Therefore, it can be concluded that statistically speaking, $\widehat{\delta^{18}\text{O}_w}$ cannot be reconstructed to a
566 precision better than $\pm 0.45\%$, while salinity cannot be reconstructed to a precision better than
567 ± 1.69 (fitting errors only) and, in reality hardly better than ± 2.65 (full to error propagation).

568

569 Finally, to complete this analysis, a direct linear fit to estimate salinity using $\exp(-\delta^{18}\text{O}_c)$
570 and Mg/Ca was performed and led to an error of ± 0.26 and a $R^2 = 0.82$ (p-value 2.10⁻⁴):

571

$$572 \quad \hat{S} = -0.16(\pm 0.02) e^{-\delta^{18}\text{O}_c} + 0.28(\pm 0.1) \frac{\text{Mg}}{\text{Ca}} + 35.80(\pm 0.33) \quad (R^2=0.81, \text{p-value} \approx 2.10^{-4}) \quad \text{Eq. 6}$$

573

574 This demonstrates that the direct reconstruction using the exact same variables as those initially
575 measured (Mg/Ca and $\delta^{18}\text{O}_c$), led to a much better estimation of salinity than the successive
576 reconstruction.

577

578

579



580 Finally, to complete this analysis, a direct linear fit to estimate salinity using $\exp(-\delta^{18}Oc)$
581 and Mg/Ca was performed and led to an error of ± 0.26 and a $R^2 = 0.82$ (p-value 2.10^{-4}):

582

583
$$\hat{S} = -0.16(\pm 0.02) e^{-\delta^{18}Oc} + 0.28(\pm 0.1) \frac{Mg}{Ca} + 35.80(\pm 0.33) \quad (R^2=0.81, \text{p-value} \approx 2.10^{-4}) \quad \text{Eq. 6}$$

584

585 This demonstrates that the direct reconstruction using the exact same variables as those initially
586 measured (Mg/Ca and $\delta^{18}Oc$), led to a much better estimation of salinity than the successive
587 reconstruction.

588

589

590

591

592

593 6. Implications

594 We analyzed shell Mg/Ca and Sr/Ca ratios, and $\delta^{18}O$ in *T. sacculifer* collected from surface
595 water along a North-South transect of the Eastern Tropical Atlantic Ocean. We find a strong
596 correlation between Mg/Ca ratios and surface water temperature, confirming the robustness of
597 surface water temperature reconstructions based on *T. sacculifer* Mg/Ca.

598 Insertion of the Sr/Ca ratio into the paleo-temperature equation improves the temperature
599 reconstruction. We established a new calibration for a paleo-temperature equation based on
600 Mg/Ca and Sr/Ca ratios for live *T. sacculifer* collected from surface water:

601

602

603

604

605
$$T = (-27 \pm 15) + (8 \pm 1) \cdot \ln(\text{Mg/Ca}) + (28 \pm 11) \cdot \text{Sr/Ca}$$

606 Scenarios were tested using previously published reconstructions. Results were compared to
607 reconstructions performed using local calibrations established in this study and therefore
608 supposed to represent the best possible calibration for this data set:

609 (1) Mg/Ca ratios measured in *T. sacculifer* specimens collected in surface water allow accurate
610 reconstruction of surface water temperature.



611 (2) $\delta_{18}O_w$ can be reconstructed with an uncertainty of $\pm 0.45\%$. Such $\delta_{18}O_w$ reconstructions
612 remain a helpful tool for paleo-reconstructions considering the global range of variation of
613 surface $\delta_{18}O_w$ (from about -7 to 2% , LeGrande and Schmidt 2006;).

614

615 (3) In contrast, the best possible salinity reconstruction based on locally calibrated equations 1,
616 4 and 5 from the present study, only allowed reconstruction with an uncertainty of ± 2.49 . Such
617 an uncertainty renders these reconstructions meaningless and does not allow for viable
618 (paleo)salinity data.

619 This is confirmed by a Monte Carlo simulation, applied to test successive reconstructions in an
620 'ideal case', where explanatory variables are known. This simulation shows that from a pure
621 statistical point of view, successive reconstructions involving Mg/Ca and $\delta_{18}O_c$ preclude
622 salinity reconstruction with a precision better than ± 1.69 and hardly better than ± 2.65 , due to
623 error propagation.

624 Nevertheless, a direct linear fit to reconstruct salinity based on the same measured variables
625 (Mg/Ca and $\delta_{18}O_c$) was established (Eq. 6) and presented in table 3. This direct reconstruction
626 of salinity should lead to a much better estimation of salinity (± 0.26) than the successive
627 reconstructions.

628

629 **ACKNOWLEDGEMENTS**

630 We thank captain and crew of the Polarstern cruise ANT XXIII/1, (Bremerhaven-Cape Town)
631 who have been of great support during this unforgettable experience. We are grateful to Susann
632 Grobe of the Marine Biogeochemistry group of the IFM-GEOMAR (Germany) for measuring
633 DIC and ALK of water samples. We thank Arnold Van Dijk of the Department of Earth
634 Sciences-Geochemistry of the University of Utrecht (The Netherlands) for measuring oxygen
635 isotope composition of water and foraminifera. We are thankful to Gijs Nobbe and Dr. Paul
636 Mason for their support with LA-ICP-MS analyses. We would like to thank Beate Mueller
637 (formally Hollmann) for her technical support when handling foraminifera, and Dr. Gernot
638 Nehrke, Dr. Stephan Mulitza, and Dr. Aurore Receveur for improving earlier versions of the
639 manuscript. We thank Prof. Dieter Wolf Gladrow for his support during the initial draft of this
640 manuscript. This work was supported by the German research foundation (DFG) under grant
641 no. BI 432/4-2 ("PaleoSalt"), and by the European Science Foundation (ESF) under the
642 EUROCORES Programme EuroCLIMATE through contract No. ERAS-CT-2003-980409 of
643 the European Commission, DG Research, FP6. Gert-Jan Reichart acknowledges funding from



644 the program of the Netherlands Earth System Science Centre (NESSC), by the Ministry of
645 Education, Culture and Science (OCW; Grant 024.002.001).

646

647

REFERENCES

648

649 Anand P, Elderfield H, and Conte MH, 2003. Calibration of Mg/Ca thermometry in planktonic
650 foraminifera from a sediment trap time series. *Paleoceanography* 18, 15. DOI:
651 10.1029/2002PA000846.

652 Anderson GM, 1976. Error propagation by the Monte Carlo method in geochemical
653 calculations, *Geochimica et Cosmochimica Acta*, Volume 40, Issue 12, 1976, Pages
654 1533-1538. DOI: 10.1016/0016-7037(76)90092-2.

655 Bahr A, Nurnberg D, Schonfeld J, Garde-Schonberg D, 2011. Hydrological variability in
656 Florida Straits during Marine Isotope Stage 5 cold events. *Paleoceanography* 26,
657 PA2214. DOI: 10.1029/2010PA002015.

658 Bé AWH, Spero HJ, and Anderson OR, 1982. The effects of symbiont elimination and
659 reinfection on the life processes of the planktonic foraminifer, *Globigerinoides*
660 *sacculifer*. *Mar. Biol.*, 70: 73-86. DOI: 10.1007/bf00397298.

661 Berger WH, 1979. Stable isotopes in foraminifera In: Lipps JH, Berger WH, Buzas MA,
662 Douglas RG, and Ross CA, Editors, *Foraminiferal Ecology and Paleoecology, SEPM*
663 *Short Course vol. 6*, Society of Economic Paleontologists and Mineralogists, Houston,
664 Texas (1979), pp. 56–91. DOI:10.2110/scn.79.06.0156.

665 Bemis BE, Spero HJ, Bijma J, Lea DW, 1998. Reevaluation of the oxygen isotopic composition
666 of planktonic foraminifera: Experimental results and revised paleotemperature
667 equations. *Paleoceanography* 13(2): 150-160. DOI: 10.1029/98PA00070.

668 Bijma J, Faber WW, and Hemleben C, 1990. Temperature and Salinity Limits for Growth and
669 Survival of Some Planktonic Foraminifera in Laboratory Cultures. *Journal of*
670 *Foraminiferal Research* 20, 95-116. DOI: 10.2113/gsjfr.20.2.95.

671 Bijma J and Hemleben C, 1993. Population-dynamics of the planktic foraminifera
672 *Globigerinoides-sacculifer* (Brady) from the central red-sea. *Deep-Sea Research Part*
673 *I-Oceanographic Research Papers* 41: 485-510. DOI: 10.1016/0967-0637(94)90092-2.

674 Bijma J, Hemleben C, and Wellnitz K, 1994. Lunar-Influenced Carbonate Flux of the Planktic
675 Foraminifer *Globigerinoides-Sacculifer* (Brady) from the Central Red-Sea. *Deep-Sea*
676 *Research Part I-Oceanographic Research Papers* 41, 511-530. DOI: 10.1016/0967-
677 0637(94)90093-0.



- 678 Cleroux C, Cortijo E, Anand P, Labeyrie L, Bassinot F, Caillon N, Duplessy JC, 2008. Mg/Ca
679 and Sr/Ca ratios in planktonic foraminifera: Proxies for upper water column temperature
680 reconstruction. *Paleoceanography* 23. DOI: 10.1029/2007PA001505.
- 681 Clifford A, 1973. Multivariate error analysis: a handbook of error propagation and calculation
682 in many-parameter systems. *John Wiley and Sons*. ISBN 978-0470160558.
- 683 Dissard D, Nehrke G, Reichart GJ, Bijma J. 2010a. The impact of salinity on the Mg/Ca and
684 Sr/Ca ratio in the benthic foraminifera *Ammonia tepida*: Results from culture
685 experiments. *Geochimica Et Cosmochimica Acta* 74: 928-940.
686 DOI: 10.1016/j.gca.2009.10.040.
- 687 Dissard D, Nehrke G, Reichart GJ, Bijma J. 2010b. Impact of seawater pCO₂ on calcification
688 and Mg/Ca and Sr/Ca ratios in benthic foraminifera calcite: results from culturing
689 experiments with *Ammonia tepida*. *Biogeosciences* 7: 81-93. DOI: 10.5194/bg-7-81-
690 2010.
- 691 Dissard D, Nehrke G, Reichart GJ, Nouet J, Bijma J. 2009. Effect of the fluorescent indicator
692 calcein on Mg and Sr incorporation into foraminiferal calcite. *Geochemistry Geophysics
693 Geosystems* 10, Q11001 DOI:10.1029/2009GC002417.
- 694 Dueñas-Bohórquez A, da Rocha RE, Kuroyanagi A, Bijma J, Reichart GJ. 2009. Effect of
695 salinity and seawater calcite saturation state on Mg and Sr incorporation in cultured
696 planktonic foraminifera. *Marine Micropaleontology* 73: 178-189.
697 DOI: 10.1016/j.marmicro.2009.09.002.
- 698 Dueñas-Bohórquez A, da Rocha RE, Kuroyanagi A, de Nooijer LJ, Bijma J, Reichart GJ. 2009.
699 Interindividual variability and ontogenetic effects on Mg and Sr incorporation in the
700 planktonic foraminifer *Globigerinoides sacculifer*. *Geochimica and cosmochimica
701 acta* 75: 520-532. DOI: 10.1016/j.gca.2010.10.006.
- 702 Eggins S, De Deckker P, Marshall J. 2003. Mg/Ca variation in planktonic foraminifera tests:
703 implications for reconstructing palaeo-seawater temperature and habitat migration.
704 *Earth and Planetary Science Letters* 212: 291-306. DOI: 10.1016/S0012-
705 821X(03)00283-8.
- 706 Elderfield H and Ganssen G, 2000. Past temperature and delta O-18 of surface ocean waters
707 inferred from foraminiferal Mg/Ca ratios. *Nature* 405, 442-445. DOI:
708 10.1038/35013033.
- 709 Emiliani C, 1954. Depth habitats of some species of pelagic foraminifera as indicated by
710 oxygen isotope ratios. *Amer J Sci*, v. 252, p. 149-158. DOI: 10.2475/ajs.252.3.149.



- 711 Epstein S, Buchsbaum R, Lowenstam HA, and Urey CH, 1953. Revised carbonate-water
712 isotopic temperature scale. *Geological Society of American Bulletin* 64, pp. 1315–1326.
713 DOI: 10.1130/0016-7606(1953)64[1315:RCITS]2.0.CO;2.
- 714 Erez J, and Luz B. 1983. Experimental Paleotemperature Equation for Planktonic-Foraminifera.
715 *Geochimica Et Cosmochimica Acta* 47, 1025-1031. DOI: 10.1016/0016-
716 7037(83)90232-6.
- 717 Friedrich O, Schiebel R, Wilson PA, Weldeab S, Beer CJ, Cooper MJ, Fiebig J. 2012. Influence
718 of test size, water depth, and ecology on Mg/Ca, Sr/Ca, $\delta_{18}\text{O}$ and $\delta_{13}\text{C}$ in nine modern
719 species of planktic foraminifers. *Earth and Planetary Science Letters* 319-320: 133-
720 145. DOI: 10.1016/j.epsl.2011.12.002.
- 721 Gaffey SJ and Bronnimann CE, 1993. Effects of Bleaching on Organic and Mineral Phases in
722 Biogenic Carbonates. *Journal of Sedimentary Petrology* 63, 752-754.
723 DOI: 10.1029/2018GC007575.
- 724 Gray WR and Evans D, 2019. Nonthermal influences on Mg/Ca in planktonic foraminifera: A
725 review of culture studies and application to the last glacial maximum.
726 *Paleoceanography and Paleoclimatology* 34, 306-315. DOI: 10.1029/2018PA003517.
- 727 Groeneveld J, Ho SL, Mackensen A, Mohtadi M, Laepple T. 2019. Deciphering the variability
728 in Mg/Ca and Oxygen Isotopes of individual foraminifera. *Paleoceanography and*
729 *Paleoclimatology* 34, 755-773. DOI: 10.1029/2018PA003533.
- 730 Hamilton CP, Spero HJ, Bijma J, Lea DW. 2008. Geochemical investigation of gametogenic
731 calcite addition in the planktonic foraminifera *Orbulina universa*. *Marine*
732 *Micropaleontology* 68: 256-267. DOI: 10.1016/j.marmicro.2008.04.003.
- 733 Hastings DW, Russell AD, and Emerson SR, 1998. Foraminiferal magnesium in
734 *Globeriginoides sacculifer* as a paleotemperature proxy. *Paleoceanography* 13, 161-
735 169. DOI: 10.1029/97PA03147.
- 736 Hemleben C, Spindler M and Anderson OR, 1989. Modern planktonic foraminifera, *Springer*
737 *Verlag, Berlin*, 363 p. ISBN 978-1-4612-3544-6.
- 738 Honisch B, Allen KA, Lea DW, Spero HJ, Eggins SM, Arbuszewski J, deMenocal P, Rosenthal
739 Y, Russell AD, Elderfield H. 2013. The influence of salinity on Mg/Ca in planktic
740 foraminifers- Evidence from cultures, core-top sediments and complementary $\delta_{18}\text{O}$.
741 *Geochimica et Cosmochimica Acta* 121: 196-213. DOI: 10.1016/j.gca.2013.07.028.
- 742 Hut G, 1987. Consultant's group meeting on stable isotope reference samples of geochemical
743 and hydrological investigations. *IAEA, Vienna*, p 42 Report to the Director General.
744 INIS-MF—10954.



- 745 Jentzen A, Nurnberg D, Hathorne EC and Schonfeld J, 2018. Mg/Ca and $\delta_{18}\text{O}$ in living planktic
746 foraminifers from the Caribbean, Gulf of Mexico and Florida Straits. *Biogeosciences*, 15,
747 7077-7095. DOI: 10.5194/bg-15-7077-2018.
- 748 Jochum KP, Weis U, Stoll B, Kuzmin D, Yang Q, Raczek I, Jacob DE, Stracke A, Birbaum K,
749 Frick DA, Gunther D, Enzweiler J, 2011. Determination of reference values for NIST
750 610-617 glasses following ISO guidelines. *Geostandards and Geoanalytical research*.
751 35, 397–429, 201. DOI: 10.1111/j.1751-908X.2011.00120.x.
- 752 Johnson KM, Wills KD, Butler DB, Johnson WK and Wong, CS, 1993. Coulometric Total
753 Carbon-Dioxide Analysis for Marine Studies - Maximizing the Performance of an
754 Automated Gas Extraction System and Coulometric Detector. *Marine Chemistry* 44,
755 167-187. DOI: 10.1016/0304-4203(93)90201-X.
- 756 Kisakurek B, Eisenhauer A, Bohm F, Garbe-Schonberg D, Erez J. 2008. Controls on shell
757 Mg/Ca and Sr/Ca in cultured planktonic foraminiferan, *Globigerinoides ruber* (white).
758 *Earth and Planetary Science Letters* 273: 260-269. DOI: 10.1016/j.epsl.2008.06.026.
- 759 Kontakiotis G, Mortyn GP, Antonarakou A, Drinia H, 2016. Assessing the reliability of
760 foraminiferal Mg/Ca thermometry by comparing field-samples and culture experiments:
761 a review. *Geological quarterly*, 2016, 60 (3): 547-560. DOI: 10.7306/gq.1272.
- 762 Langer G, Sadekov A, Thoms S, Keul N, Nehrke G, Mewes A, Greaves M, Misra S, Reichart
763 GJ, de Nooijer LJ, Bijma J, Elderfield H, 2016. Sr partitioning in the benthic
764 foraminifera *Ammonia aomoriensis* and *Amphistegina lessonii*. *Chemical Geology* 440
765 (2016) 306-312. DOI: 10.1016/j.chemgeo.2016.07.018.
- 766 Lea DW, Mashiotta TA, and Spero HJ, 1999. Controls on magnesium and strontium uptake in
767 planktonic foraminifera determined by live culturing. *Geochimica Et Cosmochimica*
768 *Acta* 63, 2369-2379. DOI: 10.1016/S0016-7037(99)00197-0.
- 769 Lear CH, Rosenthal Y, and Slowey N, 2002. Benthic foraminiferal Mg/Ca-paleothermometry:
770 A revised core-top calibration. *Geochimica Et Cosmochimica Acta* 66, 3375-3387.
771 DOI: 10.1016/S0016-7037(99)00197-0.
- 772 LeGrande AN and Schmidt GA, 2006. Global gridded data set of the oxygen isotopic
773 composition in seawater. *Geophys. Res. Lett.* 33, L12604. DOI:
774 10.1029/2006GL026011.
- 775 Mewes A, Langer G, Reichart GJ, de Nooijer LJ, Nehrke G, Bijma J, 2015. The impact of Mg
776 contents on Sr partitioning in benthic foraminifers. *Chemical Geology* 412: 92-98.
777 DOI: 10.1016/j.chemgeo.2015.06.026.



- 778 Mintrop L, Perez FF, Gonzalez-Davila M, Santana-Casiano MJ, and Kortzinger A, 2000.
779 Alkalinity determination by potentiometry: Intercalibration using three different
780 methods. *Ciencias Marinas* 26, 23-37. DOI: 10.7773/cm.v26i1.573.
- 781 Mulitza S, Boltovskoy D, Donner B, Meggers H, Paul A, and Wefer G. 2003. Temperature:
782 delta O-18 relationships of planktonic foraminifera collected from surface waters.
783 *Palaeogeography Palaeoclimatology Palaeoecology* 202, 143-152. DOI:
784 10.1016/S0031-0182(03)00633-3.
- 785 Nürnberg D, Bijma J, and Hemleben C, 1996. Assessing the reliability of magnesium in
786 foraminiferal calcite as a proxy for water mass temperatures. *Geochimica Et*
787 *Cosmochimica Acta* 60, 803-814. DOI: 10.1016/0016-7037(95)00446-7.
- 788 Nürnberg D and Groenewald J, 2006. Pleistocene variability of the Subtropical Convergence at
789 East Tasman Plateau: Evidence from planktonic foraminifera Mg/Ca (ODP Site
790 1172A). *Geochem. Geophys. Geosyst.*, 7, Q04P11, DOI:10.1029/2005GC000984.
- 791 Pahnke K, Zahn R, Elderfield H, Schulz M, 2003. 340,000-Year Centennial-Scale Marine
792 Record of Southern Hemisphere Climatic Oscillation. *Science* 15. Vol. 301, Issue
793 5635, pp. 948-952. DOI: 10.1126/science.1084451.
- 794 Paul A, Mulitza S, Pätzold J and Wolff T, 1999. Simulation of oxygen isotopes in a global
795 ocean model, from Fisher G, Wefer G. (eds), Use of Proxies in paleoceanography:
796 Examples from the South Atlantic. Springer-Verlag Berlin Heidelberg, pp 655-686.
797 DOI :10.1007/978-3-642-58646-0_27.
- 798 R Development Core Team (2019). R: A language and environment for statistical computing.
799 R Foundation for Statistical Computing, Vienna, Austria. URL [https://www.R-](https://www.R-project.org/)
800 [project.org/](https://www.R-project.org/).
- 801 Rathburn AE and DeDeckker P, 1997. Magnesium and strontium compositions of Recent
802 benthic foraminifera from the Coral Sea, Australia and Prydz Bay, Antarctica. *Marine*
803 *Micropaleontology* 32, 231-248. DOI : 10.1016/S0377-8398(97)00028-5
- 804 Regenberg M, Nurnberg D, Steph S, Groeneveld J, Garbe-Schonberg D, Tiedemann R, Dullo
805 WC, 2006. Assessing the effect of dissolution on planktonic foraminiferal Mg/Ca ratios:
806 Evidence from Caribbean core tops. *Geochemistry Geophysics Geosystems* 7. DOI :
807 10.1029/2005GC001019.
- 808 Regenberg M, Steph S, Nurnberg D, Tiedemann R, Garbe-Schonberg D, 2009. Calibrating
809 Mg/Ca ratios of multiple planktonic foraminiferal species with delta O-18-calcification
810 temperatures: Paleothermometry for the upper water column. *Earth and Planetary*
811 *Science Letters* 278: 324-336. DOI : 10.1016/j.epsl.2008.12.019.



- 812 Reichart GJ, Jorissen F, Anschutz P and Mason PRD, 2003. Single foraminiferal test chemistry
813 records the marine environment. *Geology* 31, 355-358. DOI:10.1130/0091-
814 7613(2003)031<0355:SFTCRT>2.0.CO;2.
- 815 Rohling EJ, 2000. Paleosalinity: confidence limits and future applications. *Marine Geology*
816 163, 1-11. DOI: 10.1016/S0025-3227(99)00097-3.
- 817 Rosenthal Y, Boyle EA and Labeyrie L, 1997. Last glacial maximum paleochemistry and
818 deepwater circulation in the Southern Ocean: Evidence from foraminiferal cadmium.
819 *Paleoceanography* 12, 787-796. DOI: 10.1029/97PA02508.
- 820 Sadekov A, Eggins SM, De Deckker P, Kroon D, 2008. Uncertainties in seawater thermometry
821 deriving from intratest and intertest Mg/Ca variability in *Globigerinoides ruber*.
822 *Paleoceanography* 23. DOI: 10.1029/2007PA001452.
- 823 Schmidt GA, 1999. Error analysis of paleosalinity calculations. *Paleoceanography* 14, 422-
824 429. DOI: 10.1029/1999PA900008.
- 825 Schmidt MW, Spero HJ and Lea DW, 2004. Links between salinity variation in the Caribbean
826 and North Atlantic thermohaline circulation. *Nature* 428, 160-163. DOI:
827 10.1038/nature02346.
- 828 Shackleton NJ, 1967. Oxygen isotope analyses and Pleistocene temperatures re-assessed,
829 *Nature* 215, 15–17. DOI: 10.1038/21015a0.
- 830 Shackleton NJ, 1968. Depth of Pelagic Foraminifera and Isotopic Changes in Pleistocene
831 Oceans. *Nature*, 218, 79-80. DOI : 10.1038/218079a0.
- 832 Shackleton, NJ, 1974. Attainment of isotopic equilibrium between ocean water and the
833 benthonic foraminifera genus *Uvigerina*: isotopic changes in the ocean during the last
834 glacial. *Colloques Internationaux du Centre National du Recherche Scientifique*, 219,
835 203-210. hdl:10013/epic.41396.d001.
- 836 Spero, H. J., & DeNiro, M. J. (1987). The influence of symbiont photosynthesis on the $\delta^{18}\text{O}$
837 and $\delta^{13}\text{C}$ values of planktonic foraminiferal shell calcite. *Symbiosis*, 4, 213-228.
- 838 Spero HJ, Mielke KM, Kalve EM, Lea DW and Pak DK, 2003. Multispecies approach to
839 reconstructing eastern equatorial Pacific thermocline hydrography during the past 360
840 kyr. *Paleoceanography* 18. DOI:10.1029/2002PA000814, 2003.
- 841 Spezzaferri S, Kucera M, Pearson PN, Wade BS, Rappo S, Poole CR, Morard R, Stalder C.
842 2015. *PLoS ONE*. 2015; 10 (5): e0128108. DOI: 10.1371/journal.pone.0128108.



- 843 Toyofuku T, Kitazato H, Kawahata H, Tsuchiya M, and Nohara M, 2000. Evaluation of Mg/Ca
844 thermometry in foraminifera: Comparison of experimental results and measurements in
845 nature. *Paleoceanography* 15, 456-464. DOI :10.1029/1999PA000460.
- 846 Vinogradova N, Lee T, Boutin J, Drushka K, Fournier S, Sabia R, Stammer D, Bayler E , Reul
847 N, Gordon A, Melnichenko O, Li LF, Hackert, E, Martin M, Kolodziejczyk N, Hasson
848 A, Brown S ; Misra S; Lindstrom E, 2019. Satellite Salinity Observing System: Recent
849 Discoveries and the Way Forward NASA. *Frontiers in Marine Science*. Front. Mar. Sci.
850 6: 243. DOI: 10.3389/fmars.2019.00243.
- 851 Weldeab S, Schneider RR, Kölling M and Wefer G, 2005. Holocene African droughts relate to
852 eastern equatorial Atlantic cooling. *Geology* 33, 981-984. DOI: 10.1130/G21874.1.
- 853 Weldeab S, Lea DW, Schneider RR, and Anderson N, 2007. 155,00 years of west African
854 monsoon and ocean thermal evolution. *Science* 316, 130301307.
855 DOI:10.1126/science.1140461.
- 856 World Ocean Atlas 2005, Volume 1: Temperature. S. Levitus, Ed. NOAA Atlas NESDIS 61,
857 U.S. Government Printing Office, Washington, D.C., 182 pp. NODC URL:
858 <http://www.nodc.noaa.gov/>.
- 859 Wyceh JB, Clay Kelly D, Kitajima K, Kozdon R, Orland IJ, Valley JW. 2018. Combined effects
860 of gametogenic calcification and dissolution on $\delta_{18}\text{O}$ measurements of the planktic
861 foraminifer *Trilobatus sacculifer*. *Geochemistry Geophysics Geosystems* 19, 4487-
862 4501. DOI :10.1029/2018GC007908.
- 863
864
865
866
867
868
869
870
871
872
873
874
875
876



877
 878
 879
 880
 881
 882

Table 1. Measured temperature, salinity, DIC, ALK, and $\delta_{18}\text{Ow}$ of the stations selected for this study (October/November 2005). Mean annual temperature per station (World Ocean Atlas, 2005).

Stations	Latitude	Longitude	Measured T°C (± 0.05) Oct/Nov.	Mean annual T°C	Salinity (± 0.05)	DIC ($\mu\text{mol/kg}$) precision 1 $\mu\text{m/Kg}$ accuracy 2 $\mu\text{m/Kg}$	Alkalinity ($\mu\text{mol/kg}$) precision 1.5 $\mu\text{m/Kg}$ accuracy 4 $\mu\text{m/Kg}$	$\delta_{18}\text{Ow}$ (PDB) precision 0.1 ‰ accuracy 0.2 ‰
25	22°38.640'N	20°23.578'W	24.91	21.8222	36.63	2069	2391	1.1
29	18°8.088'N	20°55.851'W	26.09	22.6964	36.24	2037	2369	0.9
31	14°32.128'N	20°57.251'W	28.24	25.0457	35.78	2009	2330	0.8
35	10°23.424'N	20°4.869'W	29.73	26.7731	35.63	1982	2304	1.2
38	7°2.114'N	17°27.818'W	29.43	27.764	34.67	1929	2257	0.7
40	4°22.323'N	15°16.911'W	28.47	27.7331	34.35	1915	2214	0.8
42	2°15.702'N	13°33.854'W	27.56	26.9215	35.72	2002	2332	1.1
46	1°35.741'S	10°33.846'W	25.91	25.6623	36.13	2053	2346	1.0
49	4°44.752'S	8°6.641'W	24.59	25.6229	36.07	2057	2369	0.9
52	8°6.086'S	5°29.077'W	23.80	24.864	35.99	2062	2360	0.7
56	11°51.783'S	2°30.743'W	22.18	23.6074	36.38	2071	2387	1.0
62	17°59.620'S	2°25.321'E	19.11	21.2856	35.99	2100	2369	1.1
66	22°26.998'S	6°6.922'E	18.71	20.1148	35.68	2070	2349	1.0

883
 884
 885
 886
 887
 888
 889
 890
 891
 892
 893
 894
 895
 896
 897



898
 899
 900
 901
 902
 903
 904

Table 2. Mean elemental (Mg/Ca and Sr/Ca) and isotopic ($\delta_{18}\text{O}_c$) composition per station, measured in foraminiferal calcite in mmol/mol and ‰ PDB, respectively. Elemental and isotopic compositions were determined on the same material (n varying from 5 to 9 specimens per station); isotopic analyses were done in duplicate for each station. Mean $\delta_{18}\text{O}_c$ - $\delta_{18}\text{O}_w$ measured per stations in ‰ PDB.

Stations	Measured Mg/Ca mmol/mol	Measured Sr/Ca mmol/mol	Measured $\delta_{18}\text{O}_c$ ‰ (V-PDB) precision 0.08‰	Measured $\delta_{18}\text{O}_c$ - $\delta_{18}\text{O}_w$ ‰ (V-PDB)	Recons. $\delta_{18}\text{O}_w$ (Mulitza) ‰ (V-PDB)	Recons. $\delta_{18}\text{O}_w$ (Spero) ‰ (V-PDB)	Recons. $\delta_{18}\text{O}_w$ (this study) ‰ (V-PDB)
25	3.22 ± 0.51	1.53 ± 0.08	-1.76	-2.82	0.38	0.40	0.88
29	4.01 ± 0.24	1.52 ± 0.06	-1.75	-2.63	1.00	0.87	1.44
31	4.78 ± 0.37	1.56 ± 0.18	-2.51	-3.33	0.73	0.49	1.11
35	5.46 ± 0.38	1.59 ± 0.08	-2.35	-3.59	1.27	0.94	1.62
38	4.31 ± 1.14	1.58 ± 0.14	-2.89	-3.59	0.07	-0.10	0.49
40	4.07 ± 0.64	1.57 ± 0.07	-2.98	-3.78	-0.18	-0.32	0.25
42	3.79 ± 0.49	1.53 ± 0.08	-2.38	-3.44	0.21	0.12	0.67
46	3.92 ± 1.24	1.47 ± 0.07	-1.67	-2.66	1.02	0.91	1.46
49	2.99 ± 0.39	1.55 ± 0.11	-1.83	-2.74	0.10	0.16	0.62
52	2.97 ± 0.30	1.50 ± 0.03	-1.34	-2.08	0.57	0.64	1.09
56	3.31 ± 0.53	1.50 ± 0.03	-1.06	-2.10	1.15	1.15	1.65
62	2.20 ± 0.24	1.47 ± 0.07	-0.70	-1.76	0.38	0.64	0.99
66	1.66 ± 0.17	1.48 ± 0.09	-0.74	-1.75	-0.46	-0.02	0.23

905
 906
 907
 908
 909
 910
 911
 912
 913
 914
 915



916
 917
 918
 919
 920

Table 3. Calibration equations for *T. sacculifer*.

Source			R ²	p-values
Mg/Ca Relationship with Temperature				
This study	Mg/Ca=0.42(±0.13)e^{(T*0.083(±0.001))}	Eq. 1	0,86	2.9e-06
Nürnberg et al., 1996	Mg/Ca=0.37(±0.065)e ^{(T*0.091(±0.007))}		0,93	
Anand et al., 2003	Mg/Ca=1.06(±0.021)e ^{(T*0.048(±0.012))}			
Regenberg et al., 2009	Mg/Ca=0.6(±0.16)e ^{(T*0.075(±0.006))}			
Sr/Ca Relationship with Temperature				
This study	Sr/Ca=(0.0094±0.002)*T+(1.29 ± 0.05)	Eq. 2	0,67	5.e-04
Mg/Ca and Sr/Ca Relationship with Temperature				
This study	T=(-27±15)+(8±1)*ln(Mg/Ca)+(28±11)*Sr/Ca	Eq. 3	0,93	2 e-04
Me/Ca Relationship with Temperature and Salinity				
This study (Mg/Ca)	ln(Mg/Ca)=(-5.10±2)+(0.09±0.009)*T+(0.11±0.05)*S		0,91	5.e-06
This study (Sr/Ca)	Sr/Ca = (1.81±0.5) + (0.008±0.002) T - (0.01±0.01)*S		0,71	0.002
δ¹⁸O Relationship with Temperature				
This study	T= 12.08(±1.46)-4.73(±0.51)*(δ¹⁸O_c -δ¹⁸O_w)	Eq. 4	0,88	1,6 e-06
Erez and Luz, (1983)	T= 16.06(±0.549)-5.08(±0.32)*(δ ¹⁸ O _c -δ ¹⁸ O _w)			
Mulitza et al., (2003)	T= 15.35(±0.71)-4.22(±0.25)*(δ ¹⁸ O _c -δ ¹⁸ O _w)			
Spero et al., (2003)	T= 12-5.67*(δ ¹⁸ O _c -δ ¹⁸ O _w)			
measured δ¹⁸O vs. measured Salinity (this study)	δ¹⁸O_w = (0.171±0.04)*S - (4.93 ±1.66)	Eq. 5	0.38	1,2 e-03
direct linear fit to reconstruct salinity based on measured variables (Mg/Ca and δ¹⁸O_c)	S = -0.16 (±0.02) e^(- δ¹⁸O_c)+ 0.28 (±0.1) Mg/Ca+35.80 (±0.33)	Eq. 6	0.82	< 2e-04

921
 922
 923
 924
 925
 926
 927
 928
 929
 930



931

932

933

934 **Table 4.** Temperature, salinity and $\delta_{18}\text{O}_w$ of the stations used to determine the salinity/ $\delta_{18}\text{O}_w$

935 relationship (equation 5)

Stations	Latitude	Longitude	T°C(±0.05)	Salinity(±0.05)	$\delta_{18}\text{O}_w$ (SMOW) precision 0.1% accuracy 0.2%
19	33°20.14'N	14°38.45'W	22,09	36,83	1,3
21	30°23.42'N	16°24.99'W	23,01	36,91	1,4
23	25°20.68'N	18°4.17'W	24,87	37,01	1,8
25	22°38.64'N	20°23.58'W	24,91	36,63	1,3
29	18°8.09'N	20°55.85'W	26,09	36,24	1,1
31	14°32.13'N	20°57.25'W	28,24	35,78	1,1
35	10°23.424'N	20°4.869'W	29,73	35,63	1,5
36	9°5.71'N	19°14.21'W	29,29	35,63	1,1
37	7°43.88'N	18°5.42'W	29,25	34,92	1,0
38	7°2.11'N	17°27.82'W	29,43	34,67	1,0
39	5°49.51'N	16°29.68'W	29,34	34,34	1,0
40	4°22.32'N	15°16.91'W	28,47	34,35	1,1
42	2°15.70'N	13°33.85'W	27,56	35,72	1,3
43	0°57.53'N	12°33.06'W	26,48	36,05	1,3
46	1°35.74'S	10°33.85'W	25,91	36,13	1,3
47	2°17.53'S	10°1.35'W	26,16	36,2	1,2
49	4°44.75'S	8°6.64'W	24,59	36,07	1,2
51	6°55.67'S	6°24.31'W	24,28	36,01	1,1
52	8°6.09'S	5°29.08'W	23,8	35,99	1,0
56	11°51.79'S	2°30.74'W	22,18	36,38	1,3
62	17°59.62'S	2°25.32'E	19,11	35,99	1,3
66	22°26.99'S	6°6.92'E	18,71	35,68	1,3
69	25°0.20'S	8°17.16'E	18,19	35,64	0,9
72	27°2.39'S	10°35.53'E	18,5	35,64	1,0

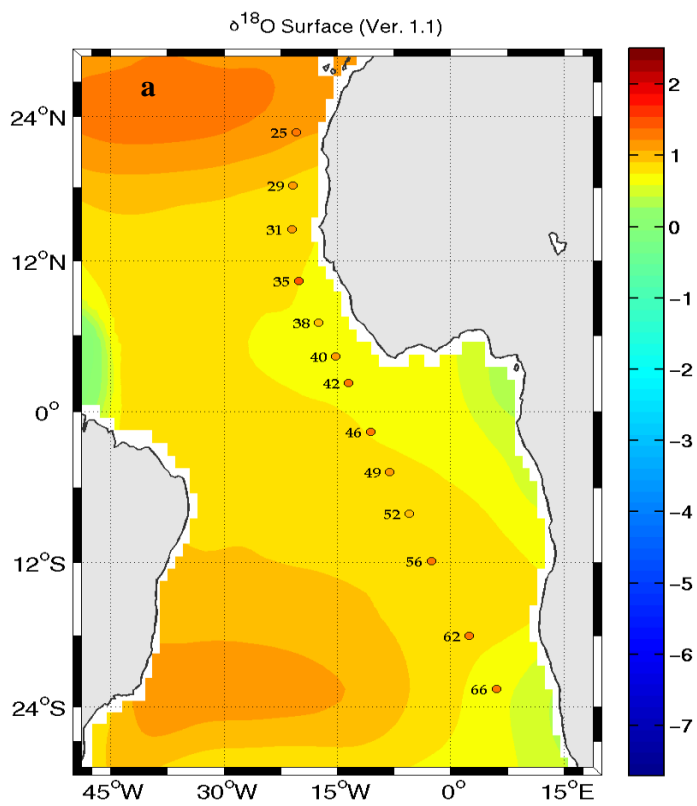
936

937

938

939

940



941



Figure 1

942

943

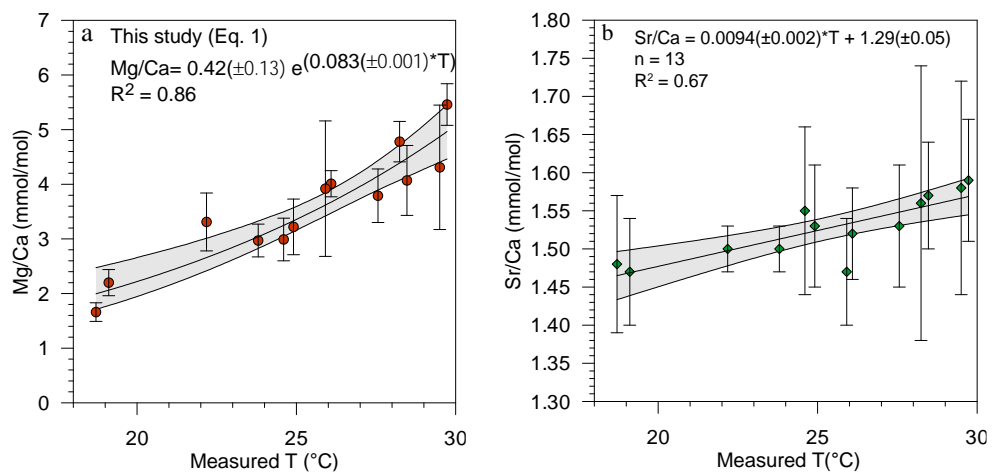
944

945

946

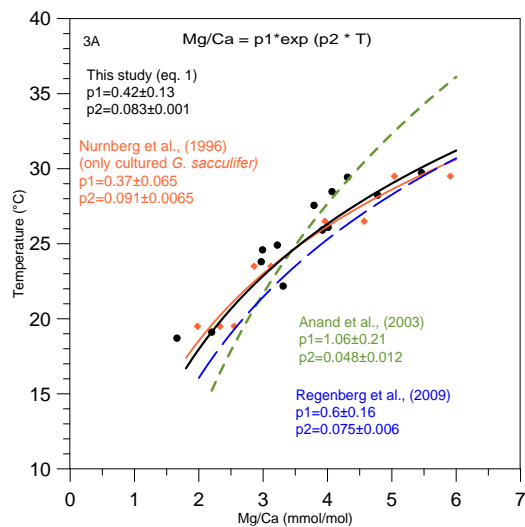


947
948



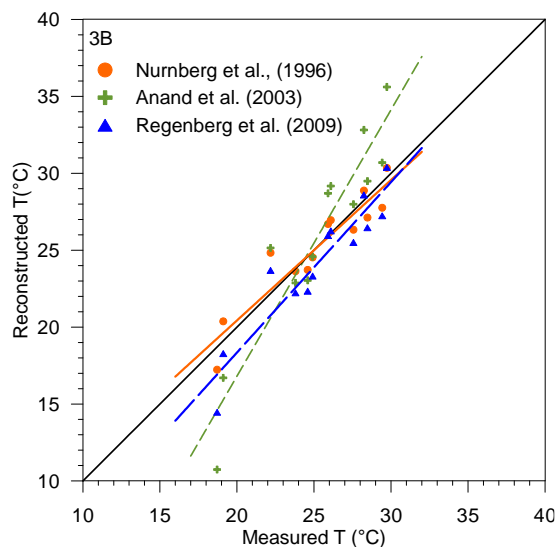
949
950
951
952
953
954
955
956
957
958
959
960
961

Figure 2



962

963



964

965

966

967

968

969

970

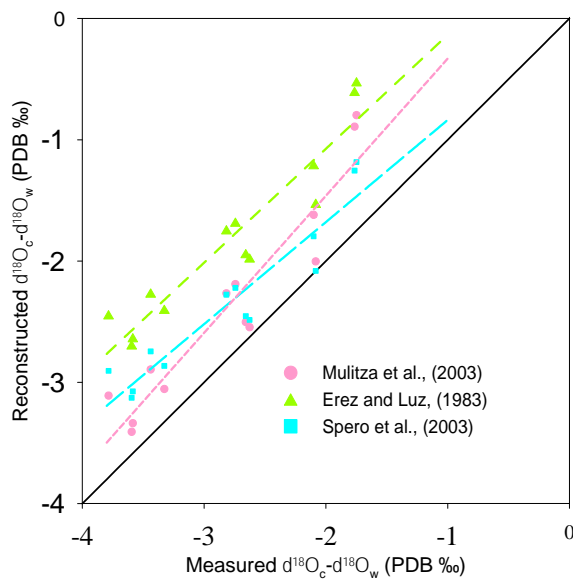
971

972

Figure 3

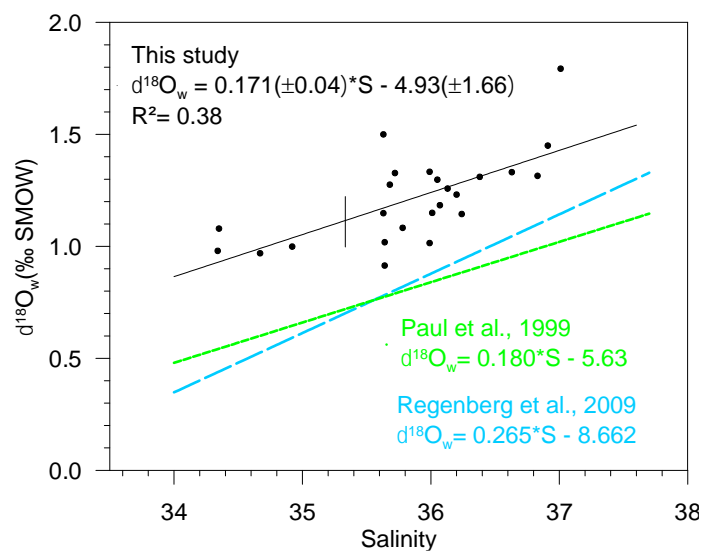


973
974



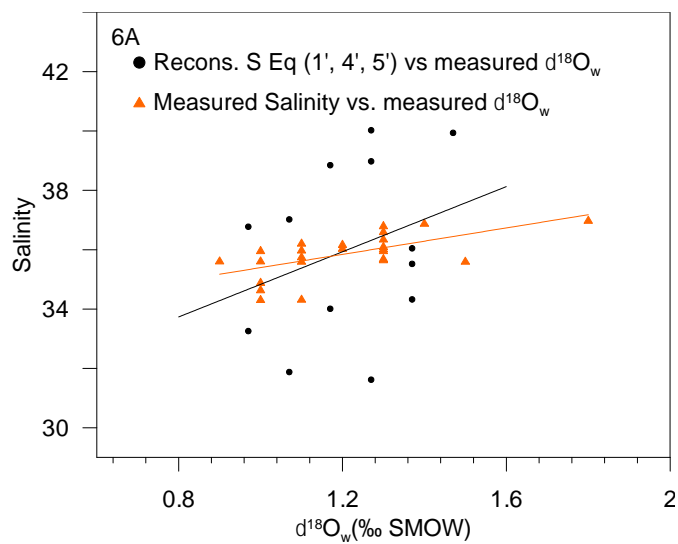
975
976
977
978
979
980
981
982
983
984
985
986
987

Figure 4

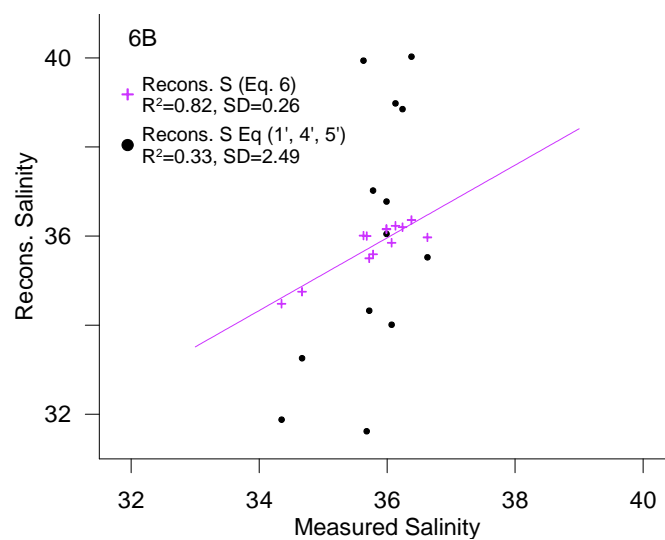


988
989
990
991
992
993
994
995
996
997
998
999
1000
1001
1002
1003
1004
1005
1006
1007

Figure 5



1008
1009
1010
1011



1012
1013
1014
1015
1016
1017
1018

Figure 6



FIGURE LEGENDS

1019

1020

1021 **Fig. 1:** Stations used in this study, plotted on gridded data set described in [LeGrande and](#)
1022 [Schmidt \(2006\)](#) (a). (<http://data.giss.nasa.gov/o18data/grid.html>). Set up for planktonic
1023 foraminifers collections (b).

1024

1025 **Fig. 2:** (a) Mg/Ca and (b) Sr/Ca (mmol/mol) and 95% confidence intervals plotted versus
1026 measured surface temperature (°C). Each point represents an average of the Mg/Ca and Sr/Ca
1027 per station.

1028

1029 **Fig. 3 a)** Mg/Paleo-temperature equations established in this study (equation 1) (black dots, and
1030 full lines), based on the data of [Nürnberg et al., \(1996\)](#) (Orange diamond and large full orange
1031 line); [Anand et al., \(2003\)](#) (small green dotted line) and [Regenberg et al., \(2009\)](#) (large blue
1032 dotted line) and **3b)** Reconstructed Mg-temperatures (Oct/Nov. 2005) plotted versus measured
1033 temperatures (°C) presented in Table 1. For each station mean measured Mg/Ca was inserted
1034 into the equation of [Nürnberg et al., \(1996\)](#) (only cultured specimens of *T. sacculifer*) (orange
1035 dots, full line), the equation of [Anand et al., \(2003\)](#) (green crosses, small dashed line), and the
1036 equation of [Regenberg et al., \(2009\)](#) (blue triangles, large dashed lines).

1037

1038 **Fig. 4:** Reconstruction of $\delta_{18}\text{O}_c - \delta_{18}\text{O}_w$ by inserting the measured temperature into three $\delta_{18}\text{O}$
1039 based paleo-T-equation: The equation of [Spero et al., \(2003\)](#) (light blue squares, large light blue
1040 dashed line), the equation of [Mulitza et al., \(2003\)](#) (pink dots, small pink dashed line), the
1041 equation sorted by [Erez and Luz \(1983\)](#) (green triangles, green dashed line) plotted versus
1042 measured $\delta_{18}\text{O}_c - \delta_{18}\text{O}_w$ (‰ PDB). The diagonal line represents the 1:1 regression.

1043

1044 **Fig. 5:** Measured surface $\delta_{18}\text{O}_w$ (‰ SMOW) plotted versus measured surface salinity (stations
1045 listed in Tab. 4) (black dots and full line). Regression lines of the $\delta_{18}\text{O}_w$ -salinity relationship
1046 calculated by [Paul et al., \(1999\)](#) for the tropical Atlantic Ocean (from 25°S to 25°N) based on
1047 GEOSECS data (green line), and by [Regenberg et al., \(2009\)](#) (blue dashed line) based on
1048 [Schmidt \(1999\)](#) data for the Atlantic Ocean for the water depth interval of 0–100 m.

1049

1050 **Fig. 6:** a) Measured salinity (orange triangles) and reconstructed salinity based on equations 1,
1051 4 and 5 from the present study (black dots), plotted versus measured $\delta_{18}\text{O}_w$.



1052 b) Reconstructed salinity based on 1) successive reconstructions using equations 1, 4 and 5
1053 from the present study (black dots) and 2) direct linear fit (Eq. 6) based on the same measured
1054 variables (Mg/Ca and $\delta^{18}O_c$) (purple crosses), plotted versus measured salinity.

1055

1056

1057

1058

1059

1060